Optical control of coherent lattice vibrations in tellurium

C. A. D. Roeser, M. Kandyla, A. Mendioroz,* and E. Mazur
Department of Physics and Division of Engineering & Applied Sciences, Harvard University, 9 Oxford Street, Cambridge, Massachusetts 02138, USA
(Received 28 September 2004; published 23 December 2004)

We present femtosecond time-resolved measurements of the dielectric tensor of tellurium under single and double pulse excitation. We demonstrate the ability to both enhance and cancel coherent lattice vibrations for large lattice shifts under near-damage threshold excitation. The excitation conditions for which cancellation is achieved in tellurium reveal a departure from the low-excitation strength behavior of similar materials.

DOI: 10.1103/PhysRevB.70.212302 PACS number(s): 63.20.−e, 78.47.+p, 77.22.Ch

Early investigations into ultrafast materials science relied on intense femtosecond laser pulses to initiate and probe dynamics that follow from photoinduced lattice instabilities.[1,2] Recently, the focus has shifted from photoinduced instabilities that lead to a disordered state[3–5] to those that result in an altered lattice configuration[6–8] and to the methods by which lattice dynamics can be controlled.[9–12] In absorbing solids, the nuclear motion is believed to follow a trajectory dictated by the potential surface of the electronic excited state,[13] much like the semiclassical picture of nuclear dynamics in molecules.[14–17]

We report the demonstration of optical control of large amplitude coherent phonons in tellurium using a two-pulse excitation scheme. Time-resolved dielectric tensor measurements reveal both the cancellation of lattice oscillations by the second excitation pulse as well as a redshift of the main resonance of the material as a result of the lattice displacement. Coupled with theoretical band structure calculations, the data provide an estimate of the size of the lattice displacement as well as the magnitude of the single-pulse-induced lattice vibration. The data also indicate a departure from the semiclassical mass-and-spring picture of the lattice dynamics observed under weak excitation.[10]

We performed pump-probe experiments on a single-crystal Czochralski-grown tellurium sample using 800-nm pulses from a multipass amplified Ti:sapphire laser, producing 0.5-mJ, 35-fs pulses at a repetition rate of 1 kHz.[18] Two collinear *s* polarized pump pulses excite the sample below the threshold for permanent damage while the *p* polarized transient reflectivity is measured using a white-light pulse (1.65−3.2 eV). Two-photon absorption measurements[19] indicate that the time-resolution of the pump-probe setup is better than 50 fs, while calculations based on measurements of the spectrum and chirp of the white-light probe indicate that the time resolution of the probe varies from 20 fs near 1.7 eV to 60 fs near 3.2 eV.[20] The entire system is calibrated to obtain absolute reflectivity. Measurements at a 68.4° and 80.4° angle of incidence, with the optic axis of Te perpendicular to the plane of incidence of the probe, allow us to determine the ordinary dielectric function $\epsilon_o(\omega)$. Measurements at the same two angles of incidence with the sample rotated so the optic axis lied within the plane of incidence allow extraction of the extraordinary dielectric function $\epsilon_e(\omega)$, given measured values of $\epsilon_o(\omega)$ at each time delay. Further details of this experimental technique can be found in Ref. 21.

Figure 1(a) shows the response of $\mathrm{Im}[\epsilon_o(\omega)]$ of Te following a single pulse excitation where the peak fluence is $0.43F_{th}$, where $F_{th}=21\ \mathrm{J/m^2}$ is the threshold fluence above which we observe visible damage to the sample. For negative time delays, when the probe arrives before the pump, the data are in excellent agreement with literature values of

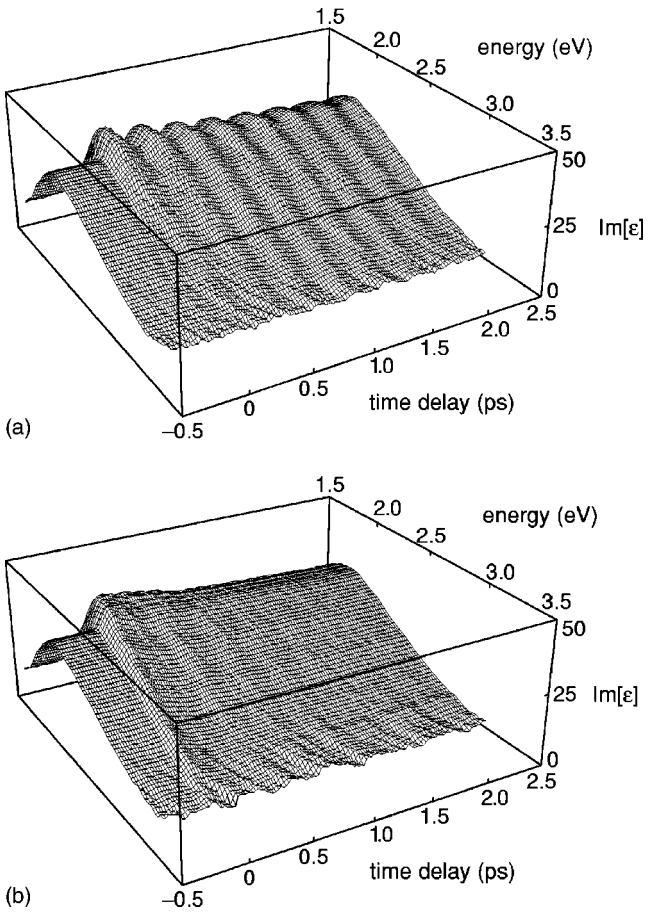

FIG. 1. Transient behavior of $\mathrm{Im}[\epsilon_o(\omega)]$ (a) under single pulse excitation at $0.43F_{th}$, and (b) under a double pulse excitation that cancels the oscillations in (a). For part (b), a $0.43F_{th}$ pulse is followed by a $0.35F_{th}$ pulse that is delayed 127 fs with respect to the first.

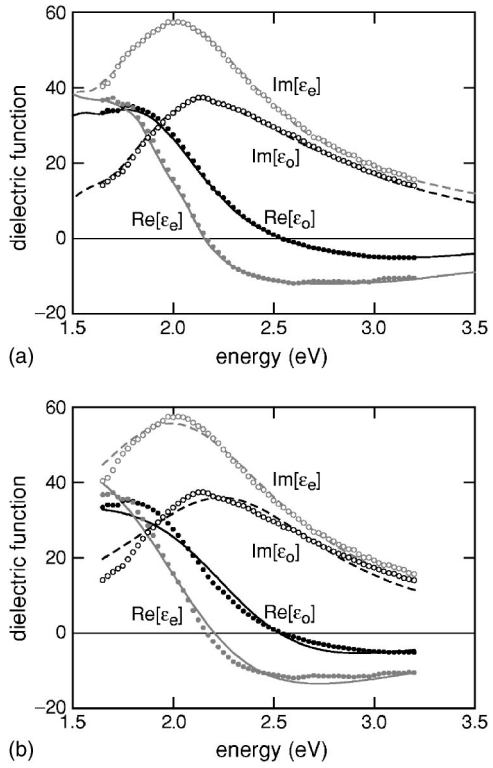

FIG. 2. (a) An agreement between measured and literature values of the dielectric tensor when the probe arrives before the pump. Measured dielectric tensor values are represented by circles, literature values are represented by curves. (b) Fits of the Drude-Lorentz model with a single resonance to the data in (a).

$\epsilon_o(\omega)$,[22] as shown in Fig. 2(a). Oscillations in the linear optical properties with a frequency >3 THz for positive time delays are due to in-phase vibrations of the A_1 phonon mode within the pumped volume.[23–25] The crystal structure of Te is that of three-atom-per-turn helices arranged on a hexagonal lattice. The lattice displacement associated with the A_1 phonon mode corresponds to a change in the helical radius that preserves the symmetry of the crystal and is confined to the plane perpendicular to the helical axis (optic axis).

Figure 1(b) shows the response of $\mathrm{Im}[\epsilon_o(\omega)]$ for a double pulse excitation where a first pump pulse at $0.43F_{\mathrm{th}}$ and a second pump pulse at $0.35F_{\mathrm{th}}$ arrive 127 fs apart. The fluence of the second pump pulse and the time delay between the exciting pulses that halts the vibrations near the first maximum displacement is uniquely determined by the fluence of the first pump pulse: oscillations in the optical properties ensue for any other second pump fluence or for any other time delay between the pump pulses.

The main feature of $\epsilon_o(\omega)$ and $\epsilon_e(\omega)$ is the broad resonance near 2 eV. Typically, each resonance in a material results from vertical transitions in one region of **k** space. Theoretical calculations show that the resonance near 2 eV is due to transitions from the uppermost valence band to the lowermost conduction band.[26,27] Other band structure calculations support this claim and further indicate that transitions of energy 2 eV are available between this valence band and the minimum of the conduction band near the A point in **k** space.[28] The simplest model that captures the contribution of all such transitions to the dielectric function is the Drude-Lorentz model,[29]

$$\epsilon(\omega) = \frac{Ne^2}{\varepsilon_0 m}\frac{1}{\omega_0^2 - \omega^2 - i\omega\Gamma}. \tag{1}$$

We applied the Drude-Lorentz model to $\epsilon_o(\omega)$ and $\epsilon_e(\omega)$ at each time delay, fitting for the resonance energy $E_{\mathrm{res}}=\hbar\omega_0$, the resonance line width $\hbar\Gamma$, and the oscillator strength $f=Ne^2/\varepsilon_0 m$. Resonances outside the spectral range of the probe give roughly constant contributions to the real part of the dielectric function within the probe range, so a real additive constant c is included in the fit to $\epsilon(\omega)$ to account for this offset. An example of the fit is shown in Fig. 2(b) for a time delay of -300 fs. The parameters of the fit are $f=110$, $E_{\mathrm{res}}=2.33$ eV, $\hbar\Gamma=1.34$ eV, and $c=7.34$ for the ordinary part and $f=161$, $E_{\mathrm{res}}=2.11$ eV, $\hbar\Gamma=1.41$ eV, and $c=5.77$ for the extraordinary part. The differences in the fit values for $\epsilon_o(\omega)$ and $\epsilon_e(\omega)$ are due to the differences in $\epsilon_o(\omega)$ and $\epsilon_e(\omega)$ themselves; the variation in the matrix elements of the dipole interaction that couples the same set of states when the electric field is parallel or perpendicular to the optic axis results in slightly different optical properties.

The Drude-Lorentz fits to the time-resolved dielectric tensor data show that all four fit parameters deviate from their pre-excitation values for positive time delays. Statistical tests of the fit question the significance of the variation in the additive constant c and no consistent behavior is observed in its dynamics. On the other hand, the oscillator strength f and the line width $\hbar\Gamma$ increase somewhat upon excitation for both the ordinary and extraordinary dielectric functions. The change in the resonance energy E_{res} is the most statistically significant feature of the dynamics as well as that of the greatest physical significance.

Figure 3 shows the changes in the resonance energy obtained from fits to $\epsilon_o(\omega)$ and $\epsilon_e(\omega)$ under various single and double pulse excitation conditions. In all parts, pump pulses "1" and "2" (and "3") indicate their time of arrival and their 35-fs pulse duration is drawn to scale. In Fig. 3(a), the variation in the resonance energy in $\epsilon_o(\omega)$ is shown under single pulse excitation at $0.57F_{\mathrm{th}}$ and under double pulse excitation at $0.57F_{\mathrm{th}}$ and $0.46F_{\mathrm{th}}$ with a pulse separation of 133 fs. The data show that this double pulse combination leads to cancellation of the coherent phonons. The cancellation of oscillations in the $\epsilon_e(\omega)$ data is shown in parts (b) and (c) under different excitation conditions. Figure 3(b) shows single pulse oscillations, double pulse cancellation, and double pulse enhancement of the oscillations for a first pump pulse fluence of $0.43F_{\mathrm{th}}$ and a second pump pulse fluence of $0.33F_{\mathrm{th}}$. For cancellation, the time delay between pump pulses is 127 fs, while for maximum enhancement the time delay is 267 fs. Figure 3(c) shows cancellation at the first maximum as well as at the second maximum, both leading to roughly the same lattice displacement for different excitations ($1=0.57F_{\mathrm{th}}$, $2=0.45F_{\mathrm{th}}$, 133 fs delay for first-maximum cancellation; $1=0.71F_{\mathrm{th}}$, $2=0.34F_{\mathrm{th}}$, 467 fs delay for second-maximum cancellation).

Using density functional theory calculations of the band structure,[28,30] we can estimate the size of the lattice displace-

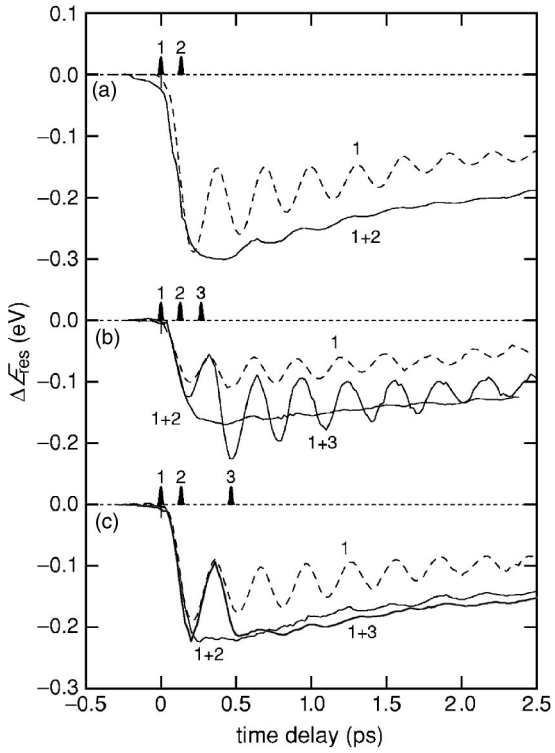

FIG. 3. Transient behavior of the main resonance energy determined by Drude-Lorentz fits to the data. (a) Pump pulses 1 and 2 lead to cancellation of the oscillations at the first peak. By varying the time delay between the two pump pulses, enhancement [(b), "1+3"] or cancellation at later peaks [(c), "1+3"] can be achieved.

ment from the measured changes in the resonance energy. The energy gap between valence and conduction bands that give rise to the resonance near 2 eV depends on the helical radius as $\Delta E_{\mathrm{res}} \approx -20\ \mathrm{eV}/\Delta u$,[30] where u is the ratio of the helical radius to the spacing of the helices on the hexagonal array, a. The equilibrium lattice parameters are $u=0.2633$ and $a=0.4456$ nm. The data in Figs. 3(a) and 3(c) represent the maximum displacement that can be achieved under double pulse excitation without causing permanent damage to the sample. Given that the resonance shifts by approximately −0.2 eV, the maximum controllable lattice displacement is approximately $\Delta u/u \approx 0.04$, which corresponds to an increase of 0.004 nm in the helical radius. Under $0.85F_{\mathrm{th}}$ single pulse excitation, tellurium shows a 0.15-eV peak-to-trough oscillation of the resonance energy, or a 0.003-nm coherent phonon amplitude.

Many aspects of the current theoretical understanding of coherent phonon excitation in absorbing solids are supported by the results presented here. Both the *displacive excitation of coherent phonons* theory[31] and the *light-excitation of coherent phonon* theory[32] predict that the coherent phonons are driven by deformation potential-coupling of the excited electrons. In essence, photoexcitation breaks a number of bonds in the material and the nuclear motion that ensues follows a classical trajectory on the potential energy surface determined by the number (and distribution) of the excited carriers. In zincblende semiconductors, calculations show that the absorption of intense femtosecond pulses can produce a potential surface with no minimum, leading to disorder within hundreds of femtoseconds.[13] In tellurium, density functional theory calculations show that transferring electrons from the valence band to the conduction band changes the potential surface so that a larger equilibrium helical radius is established.[28]

Given that the distribution of excited carriers drives the coherent phonons, the process of coherent control can be thought of in the following way. The first pump pulse establishes a new potential surface on which the nuclei move. Initially displaced from the newly established equilibrium configuration, the lattice achieves this configuration in approximately one quarter of a phonon period, but the nuclei have momentum at that point. When the nuclei reach the classical turning point of their motion, a second pump pulse can excite the precise density of carriers to shift the equilibrium position to the current position of the ions, stopping the oscillatory motion. Because photoexcitation of additional electrons can only increase the equilibrium helical radius, the vibrations can only be stopped at the maximum displacement. For weak excitation pulses, cancellation of the coherent vibrations at the maximum displacement has been observed in bismuth films.[10]

In contrast to the low excitation results, our experiments reveal that under strong excitation the vibrations do not stop at the maximum displacement. The 127 fs and 133 fs time delays that achieve cancellation as shown in Fig. 3 do not coincide with the time to reach the maximum displacement in the single pump case, which is approximately 220 fs. The 467 fs time delay between pulses that results in cancellation near the second maximum is also smaller than the 520 fs it takes for the ions to reach the second maximum under single pulse excitation. Similar results occur in bismuth under strong excitation, where a 500 fs delay between pump pulses cancelled the lattice vibrations near the second maximum, while the second maximum is reached 600 fs after single pulse excitation,[12] but the authors do not comment on the discrepancy. Our dielectric tensor data reveal that the resonance energy redshifts beyond the single pump maximum for phonon-cancelling excitations, as shown in Fig. 3. Thus, in addition to the delay between pulses being different from expected, the nuclei do not stop their coherent oscillations at the classical turning point, which is also different from the low-excitation strength behavior of other materials.[10]

The fact that the second pump pulse causes the ions to move past the classical turning point without resulting in oscillations indicates that the value of the equilibrium helical radius continues to change after the second pump has been fully absorbed. This departure of the molecular dynamics from that of an impulsively driven mass-spring system is the manifestation of a time-dependent driving term, i.e., that the carrier-lattice coupling through the deformation potential changes in time. The difference between the tellurium lattice dynamics and that of a mass-spring system are also apparent in the single-pulse excitation data where the first maximum is reached at 220 fs rather than at one half of the 310-fs phonon period [see Fig. 3(a)]. The physical origin of such a phenomenon would likely involve many body effects, such as a deformation coupling that changes with lattice configuration. For a sufficiently large displacement of the lattice, a

further increase in the helical radius may allow the excited electrons to redistribute in such a way as to increase the equilibrium helical radius. In this way, the lattice essentially "pulls" the equilibrium position along until it costs too much energy to displace the lattice further, at which point the helices stop their expansion and slowly return to their unexcited configuration.

The dynamics of tellurium under near-damage threshold excitation illustrate an interesting dynamic relationship between the excited carriers that drive the lattice motion and the lattice whose configuration determines the band structure on which the carriers redistribute. The observation of this effect only at large ionic displacements and high excited carriers further supports the notion that many-body effects play an important role in determining the system dynamics. While the subject of coherent phonons has enjoyed a great deal of theoretical inquiry,[28,31–33] our results invite new investigation of the interplay between excited carriers and lattice motion.

We gratefully acknowledge P. Grosse for providing tellurium samples and P. Tangney, S. Fahy, N. Choly, and E. Kaxiras for discussions. A.M. acknowledges financial support from the Basque Country Government through the Research Staff Mobility Program, B.1. This work was supported by the NSF under Grant No. DMR-0303642.

*Also at the Departamento de Física Aplicada I, Universidad del País Vasco, Escuela Superior de Ingenieros, Alda. Urquijo s/n, 48013 Bilbao, Spain.

[1] C. V. Shank, R. Yen, and C. Hirlimann, Phys. Rev. Lett. **50**, 454 (1983).
[2] C. V. Shank, R. Yen, and C. Hirlimann, Phys. Rev. Lett. **51**, 900 (1983).
[3] P. Saeta, J.-K. Wang, Y. Siegal, N. Bloembergen, and E. Mazur, Phys. Rev. Lett. **67**, 1023 (1991).
[4] S. V. Govorkov, I. L. Shumay, W. Rudolph, and T. Schröder, Opt. Lett. **16**, 1013 (1991).
[5] K. Sokolowski-Tinten, H. Schulz, J. Bialkowski, and D. von der Linde, Appl. Phys. A: Solids Surf. **53**, 227 (1991).
[6] O. V. Misochko, M. Tani, K. Sakai, S. Nakashima, V. N. Andreev, and F. A. Chudnovsky, Physica B **263-264**, 57 (1999).
[7] A. Cavalleri, C. Tóth, C. W. Siders, J. A. Squier, F. Ráski, P. Forget, and J. C. Kieffer, Phys. Rev. Lett. **87**, 237401 (2001).
[8] K. Sokolowski-Tinten, C. Blome, J. Blums, A. Cavalleri, C. Dietrich, A. Tarasevitch, I. Uschmann, E. Förster, M. Kammler, M. Horn-von-Hoegon *et al.*, Nature (London) **81**, 3679 (1998).
[9] M. W. Wefers, H. Kawashima, and K. A. Nelson, J. Phys. Chem. Solids **57**, 1425 (1995).
[10] M. Hase, K. Mizoguchi, H. Harima, S. Nakashima, M. Tani, K. Sakai, and M. Hangyo, Appl. Phys. Lett. **69**, 2474 (1996).
[11] A. Bartels, T. Dekorsy, H. Kurz, and K. Köhler, Appl. Phys. Lett. **72**, 2844 (1998).
[12] M. F. DeCamp, D. A. Reis, P. H. Bucksbaum, and R. Merlin, Phys. Rev. B **64**, 092301 (2001).
[13] P. Stampfli and K. H. Bennemann, Phys. Rev. B **49**, 7299 (1994).
[14] E. J. Heller, J. Chem. Phys. **68**, 2066 (1978).
[15] D. J. Tannor, R. Kosloff, and S. A. Rice, J. Chem. Phys. **85**, 5805 (2086).
[16] A. Assion, T. Baumert, J. Helbing, V. Seyfried, and G. Gerber, Chem. Phys. Lett. **259**, 488 (1996).
[17] T. Brixner, N. H. Damrauer, P. Niklaus, and G. Gerber, Nature (London) **414**, 57 (2001).
[18] S. Backus, J. Peatross, C. P. Huang, M. M. Murnane, and H. C. Kapteyn, Opt. Lett. **20**, 2000 (1995).
[19] T. F. Albrecht, K. Seibert, and H. Kurz, Opt. Commun. **84**, 223 (1991).
[20] S. A. Kovalenko, A. L. Dobryakov, J. Ruthmann, and N. P. Ernsting, Phys. Rev. A **59**, 2369 (1999).
[21] C. A. D. Roeser, A. M.-T. Kim, J. P. Callan, L. Huang, E. N. Glezer, Y. Siegal, and E. Mazur, Rev. Sci. Instrum. **74**, 3413 (2003).
[22] E. D. Palik, *Handbook of Optical Constants of Solids* (Academic Press, New York, 1985).
[23] H. J. Zeiger, J. Vidal, T. K. Cheng, E. P. Ippen, G. Dresselhaus, and M. S. Dresselhaus, Phys. Rev. B **45**, 768 (1992).
[24] S. Hunsche, K. Wienecke, T. Dekorsy, and H. Kurz, Phys. Rev. Lett. **75**, 1815 (1995).
[25] A. M.-T. Kim, C. A. D. Roeser, and E. Mazur, Phys. Rev. B **68**, 012301 (2003).
[26] J. Maschke, Phys. Status Solidi B **47**, 511 (1971).
[27] H. M. Isomäki, J. von Boehm, and T. Stubb, Phys. Rev. B **26**, 5815 (1982).
[28] P. Tangney and S. Fahy, Phys. Rev. B **65**, 054302 (2002).
[29] N. W. Ashcroft and N. D. Mermin, *Solid State Physics* (Saunders College, Philadelphia, 1976).
[30] P. Tangney, Master's thesis, University College Cork, Ireland, 1998.
[31] A. V. Kuznetsov and C. J. Stanton, Phys. Rev. Lett. **73**, 3243 (1994).
[32] R. Merlin, Solid State Commun. **102**, 207 (1997).
[33] P. Tangney and S. Fahy, Phys. Rev. Lett. **82**, 4340 (1999).